

# Online Research @ Cardiff

This is an Open Access document downloaded from ORCA, Cardiff University's institutional repository: <https://orca.cardiff.ac.uk/id/eprint/104398/>

This is the author's version of a work that was submitted to / accepted for publication.

Citation for final published version:

Demenev, A. A., Kulakovskii, V. D., Schneider, C., Brodbeck, S., Kamp, M., Höfling, S., Lobanov, Sergey ORCID: <https://orcid.org/0000-0002-3126-1903>, Weiss, T., Gippius, N. A. and Tikhodeev, S. G. 2016. Circularly polarized lasing in chiral modulated semiconductor microcavity with GaAs quantum wells. Applied Physics Letters 109 (17) , 171106. 10.1063/1.4966279 file

Publishers page: <http://dx.doi.org/10.1063/1.4966279>  
<<http://dx.doi.org/10.1063/1.4966279>>

Please note:

Changes made as a result of publishing processes such as copy-editing, formatting and page numbers may not be reflected in this version. For the definitive version of this publication, please refer to the published source. You are advised to consult the publisher's version if you wish to cite this paper.

This version is being made available in accordance with publisher policies.

See

<http://orca.cf.ac.uk/policies.html> for usage policies. Copyright and moral rights for publications made available in ORCA are retained by the copyright holders.



## Circularly polarized lasing in chiral modulated semiconductor microcavity with GaAs quantum wells

A. A. Demenev, V. D. Kulakovskii, C. Schneider, S. Brodbeck, M. Kamp, S. Höfling, S. V. Lobanov, T. Weiss, N. A. Gippius, and S. G. Tikhodeev

Citation: *Appl. Phys. Lett.* **109**, 171106 (2016); doi: 10.1063/1.4966279

View online: <http://dx.doi.org/10.1063/1.4966279>

View Table of Contents: <http://aip.scitation.org/toc/apl/109/17>

Published by the [American Institute of Physics](#)

---

### Articles you may be interested in

[Synthetic hybrid Co<sub>2</sub>FeGe/Ge\(Mn\) superlattice for spintronics applications](#)

*Applied Physics Letters* **109**, 172401 (2016); 10.1063/1.4965977

[Laser-generated focused ultrasound for arbitrary waveforms](#)

*Applied Physics Letters* **109**, 174102 (2016); 10.1063/1.4964852

[An optically pumped 2.5  \$\mu\text{m}\$  GeSn laser on Si operating at 110 K](#)

*Applied Physics Letters* **109**, 171105 (2016); 10.1063/1.4966141

[Impact of oxygen stoichiometry on electroforming and multiple switching modes in TiN/TaO<sub>x</sub>/Pt based ReRAM](#)

*Applied Physics Letters* **109**, 173503 (2016); 10.1063/1.4965872

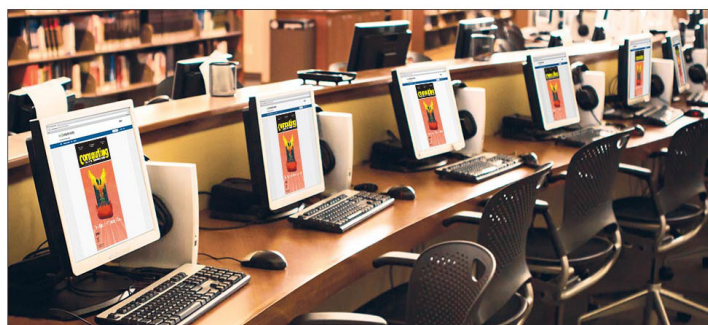
[On Mott-Schottky analysis interpretation of capacitance measurements in organometal perovskite solar cells](#)

*Applied Physics Letters* **109**, 173903 (2016); 10.1063/1.4966127

[Thermodynamic efficiency limits of classical and bifacial multi-junction tandem solar cells: An analytical approach](#)

*Applied Physics Letters* **109**, 173504 (2016); 10.1063/1.4966137

---



CiSE is already at  
your fingertips...



In the IEEE Xplore and  
AIP library packages.

# Circularly polarized lasing in chiral modulated semiconductor microcavity with GaAs quantum wells

A. A. Demenev,<sup>1</sup> V. D. Kulakovskii,<sup>1</sup> C. Schneider,<sup>2</sup> S. Brodbeck,<sup>2</sup> M. Kamp,<sup>2</sup> S. Höfling,<sup>2,3</sup> S. V. Lobanov,<sup>4</sup> T. Weiss,<sup>5</sup> N. A. Gippius,<sup>6,7</sup> and S. G. Tikhodeev<sup>1,7,8,a)</sup>

<sup>1</sup>*Institute of Solid State Physics, Russian Academy of Science, Chernogolovka 142432, Russia*

<sup>2</sup>*Technische Physik and Wilhelm-Conrad-Röntgen-Research Center for Complex Material Systems, Universität Würzburg, Am Hubland, Würzburg D-97074, Germany*

<sup>3</sup>*SUPA, School of Physics and Astronomy, University of St Andrews, St Andrews, KY16 9SS, United Kingdom*

<sup>4</sup>*School of Physics and Astronomy, Cardiff University, Cardiff CF24 3AA, United Kingdom*

<sup>5</sup>*4th Physics Institute and Research Center SCoPE, University of Stuttgart, Stuttgart D-70550, Germany*

<sup>6</sup>*Skolkovo Institute of Science and Technology, Novaya Street 100, Skolkovo 143025, Russia*

<sup>7</sup>*A. M. Prokhorov General Physics Institute, Russian Academy of Sciences, Vavilova Street 38, Moscow 119991, Russia*

<sup>8</sup>*M. V. Lomonosov Moscow State University, Leninskie Gory 1, Moscow 119991, Russia*

(Received 29 July 2016; accepted 12 October 2016; published online 27 October 2016)

We report close to circularly polarized lasing at  $\hbar\omega = 1.473$  and  $1.522$  eV from an AlAs/AlGaAs Bragg microcavity, with 12 GaAs quantum wells in the active region and chirally etched upper distributed Bragg refractor under optical pump at room temperature. The advantage of using the chiral photonic crystal with a large contrast of dielectric permittivities is its giant optical activity, allowing to fabricate a very thin half-wave plate, with a thickness of the order of the emitted light wavelength, and to realize the monolithic control of circular polarization. *Published by AIP Publishing.* [<http://dx.doi.org/10.1063/1.4966279>]

Modern nanofabrication technologies allow to realize photonic structures—photonic crystals and metamaterials—with extraordinary optical properties.<sup>1–3</sup> In particular, chiral photonic structures are known to demonstrate a giant optical activity, several orders of magnitude stronger than natural materials.<sup>4–9</sup> Recently, it has been demonstrated that incorporating a chiral photonic structure into a planar GaAs waveguide or a semiconductor microcavity (MC) with embedded light-emitting achiral InAs quantum dots (QDs) allows to achieve light emission with a high degree of circular polarization (DCP), without applying magnetic field and without the need of thick quarter-waveplates.<sup>10–12</sup> The effect is due to the modification of the symmetry and density of environmentally allowed electromagnetic modes relative to that in free space due to the chiral nanostructuring, which, in turn, affects the spontaneous emission rate, directional pattern, and polarization.<sup>13,14</sup> This method has considerable advantages: small size, very simple operation, and compatibility with semiconductor fabrication process. In this Letter, we demonstrate that the method works for the stimulated emission as well, and demonstrate a highly circularly polarized lasing from an AlGaAs/AlAs microcavity with chirally etched top Bragg mirror with GaAs quantum wells (QWs) in the active cavity. Previously, the elliptically polarized lasing with a good DCP was realized on a quantum cascade laser with monolithic control of circular polarization in the THz range of frequencies.<sup>15</sup>

A chiral photonic crystal (CPC), a monolithic part of the upper cavity mirror, is fabricated from the AlAs/AlGaAs/GaAs high Q-factor MC grown by molecular beam epitaxy on a (001)-oriented GaAs. The full planar cavity consists of

a lower and an upper Bragg reflectors with 27 and 23 pairs of AlAs/Al<sub>0.20</sub>Ga<sub>0.80</sub>As layers, respectively, with 3 nm GaAs smoothing layer after each pair in the Bragg reflectors and an active layer with three groups of four 13 nm GaAs QWs separated by 4 nm AlAs barriers. The nominal thicknesses of the AlAs and Al<sub>0.20</sub>Ga<sub>0.80</sub>As layers in Bragg mirrors are  $(68 \pm 3)$  nm and  $(58 \pm 3)$  nm, respectively. The Bragg pairs are deposited on the wafer with a slight wedge from the center to the circumference, resulting in a blueshift of the cavity resonance that can amount up to  $\approx 200$  meV. It consists of the central group of four GaAs QWs with three AlAs barriers between them, surrounded by 32 nm AlAs and 26 nm Al<sub>0.20</sub>Ga<sub>0.80</sub>As layers, and symmetric siding groups of four AlAs/GaAs barrier/QW layers with 28 nm AlAs trailing layers, see the [supplementary material](#).

A chiral layer is fabricated by electron-beam nanolithography and dry etching through top  $N_{\text{etch}} = 4.75$  Bragg pairs of the upper mirror (which means through the four top Bragg pairs, the AlAs layer, and 1/2 of the Al<sub>0.20</sub>Ga<sub>0.80</sub>As layer of the 5th Bragg pair). The schematics of the CPC is depicted in Fig. 1, see also the [supplementary material](#). It consists of a square lattice of rectangular pillars that have a broken in-plane mirror symmetry but possess a fourfold rotational axis and provides strong optical activity.<sup>16</sup> The vertical walls of nanopillars are normal to the [110] and  $\bar{1}10$  crystallographic directions. This structure has a  $C_4$  point symmetry, and it is three-dimensionally chiral, because it does not have planes of mirror symmetry, including the horizontal one.<sup>6</sup>

Two different periodic structures (Samples A and B hereafter) have been fabricated, based on the theoretical calculations explained below and shown schematically in Figs. 1(a) and 1(b). Sample A (panel a) has period  $p = 1060$  nm and pillar feature size  $L = 544$  nm, and Sample B (panel b) has

<sup>a)</sup>tikh@gpi.ru



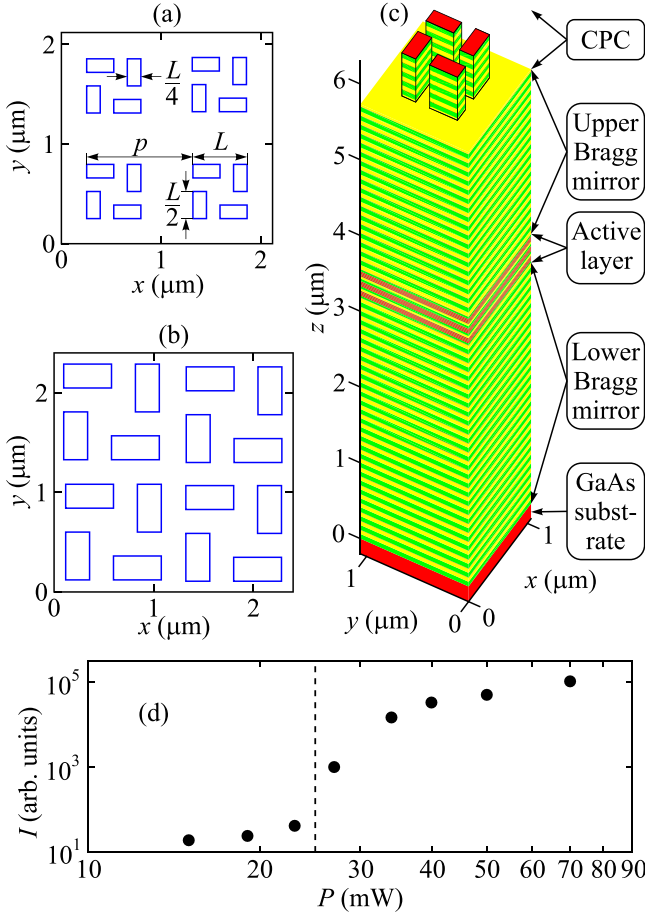


FIG. 1. (a and b) The schematics of chiral photonic crystal (CPC) composed of a square lattice of rectangular nanopillars in Samples A (panel (a)) and B (panel (b)),  $2 \times 2$  periods are shown. (c) Schematics of the unit cell of Sample A. The nanopillars, composing the CPC, are etched through the top 4.75 (of 23) Bragg pairs of the upper Bragg mirror of a planar AlGaAs/AlAs microcavity with twelve GaAs QWs (three groups of four). Green and yellow colors represent AlAs and AlGaAs  $\lambda/4$ -layers, respectively. Red color represents the GaAs substrate, smoothing layers between Bragg pairs and active QWs. (d) Measured (for Sample A) emission intensity  $I$  as a function of the optical pump intensity  $P$ .

$p = 1200 \text{ nm}$  and  $L = 960 \text{ nm}$ . The horizontal size of chiral structure in each sample is approximately  $50 \times 50 \mu\text{m}^2$ . Samples A and B are cleaved from different horizontal parts of the wafer, and show different photon energies of the main MC mode, around 1523 and 1473 meV at room temperature, respectively.

The samples are held at room temperature. The excitation is carried out with a Ti-sapphire laser in the spectral range of the first reflection minimum of the MC. The laser spot has a diameter of about  $10 \mu\text{m}$ . The emission is collected in an angle range of  $\pm 15^\circ$ . It is dispersed by a monochromator and detected by a Si CCD camera. The polarization of the luminescence is analyzed by a quarter wave retarder and linear polarizers.

The emission intensity from both samples at low pump intensities depends weakly on the angle, its spectral width reaches a few meV. With an increase in the excitation power, the emission spectrum and intensity show a threshold-like transition to lasing regime at  $P = P_{\text{thr}}$ , see Fig. 1(d) for Sample A. Above the threshold, the emission line becomes narrow. The full width at half maximum is about 0.23 meV

at  $P = 1.1P_{\text{thr}}$  and increases to  $\sim 0.5 \text{ meV}$  at  $P = 2.5P_{\text{thr}}$ . Figures 2(a) and 2(b) display the measured emission intensities (from Samples A and B, respectively) in two circular ( $I^+$ ,  $I^-$ ) and two linear ( $I^x$ ,  $I^y$ ) polarizations as functions of photon energy  $\hbar\omega$ , at the normal to the MC plane at  $P \sim 2P_{\text{thr}}$  and zero magnetic field. (The emission intensities in two diagonal linear polarizations  $x \pm y$  are not shown as they differ very weakly from each other.) The dashed lines in Figs. 2(a) and 2(b) show the degrees of circular, linear, and total polarization defined as

$$\rho_c = \frac{I^+ - I^-}{I^+ + I^-}, \quad \rho_{xy} = \frac{I^x - I^y}{I^x + I^y}, \quad \rho_{x \pm y} = \frac{I^{x+y} - I^{x-y}}{I^{x+y} + I^{x-y}},$$

$$\rho_{\text{lin}} = \sqrt{\rho_{xy}^2 + \rho_{x \pm y}^2}, \quad \rho_{\Sigma} = \sqrt{\rho_c^2 + \rho_{\text{lin}}^2}. \quad (1)$$

It is seen that in Sample A the lasing is nearly completely elliptically polarized, with polarization degrees at the intensity maxima as large as  $\rho_c \sim 80\%$ ,  $\rho_{\text{lin}} \sim 50\%$ , and  $\rho_{\Sigma} \sim 95\%$  (Fig. 2(a)). The polarization of emission in Sample B (Fig. 2(b)) is smaller,  $\rho_c \sim 60\%$ ,  $\rho_{\text{lin}} \sim 35\%$ , and  $\rho_{\Sigma} \sim 80\%$ . This is in agreement with a significantly broader linewidth of the emission from Sample B, compare Figs. 2(a) and 2(b).

The reciprocity and symmetry analysis of the structure shows that the CPC in the structures works as a waveplate, exploring the Fabry-Perot interference between the vertically propagating modes in the slab, which allows reaching nearly a 100% circular polarization of the transmission.<sup>11</sup> To optimize the chiral structures for obtaining a high DCP of light emission, we have calculated the frequency dependence of

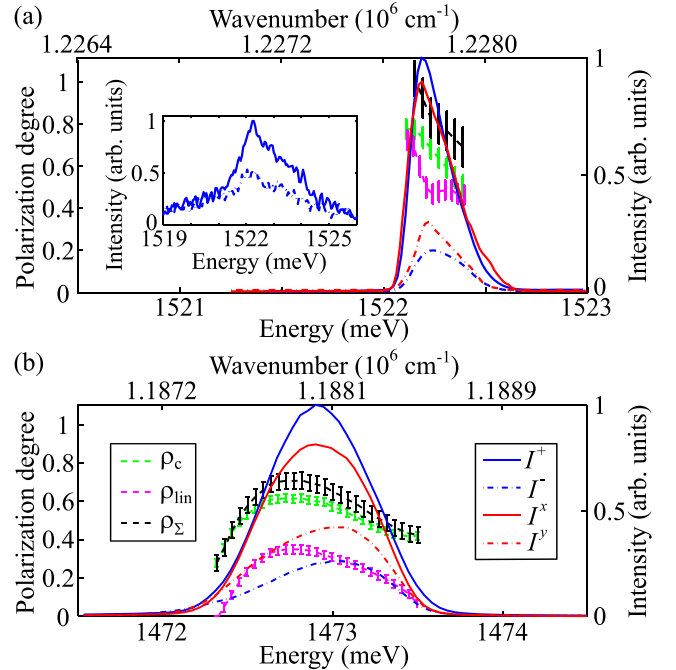


FIG. 2. (a) Emission intensity spectra of Sample A at  $T = 300 \text{ K}$  at pump intensity above the threshold, at  $P \approx 2P_{\text{thr}}$ , in circular  $I^\pm$  (blue solid and dashed-dotted lines) and linear  $I^{x,y}$  (red lines) polarizations. Green, magenta, and black lines with errorbars show the circular, linear, and total polarization degrees,  $\rho_c$ ,  $\rho_{\text{lin}}$ ,  $\rho_{\Sigma}$ , respectively. (b) Same for Sample B. The inset in panel (a) shows the emission spectra in circular polarizations  $I^\pm$  in Sample A slightly below the threshold, at  $P = 0.95P_{\text{thr}}$ .

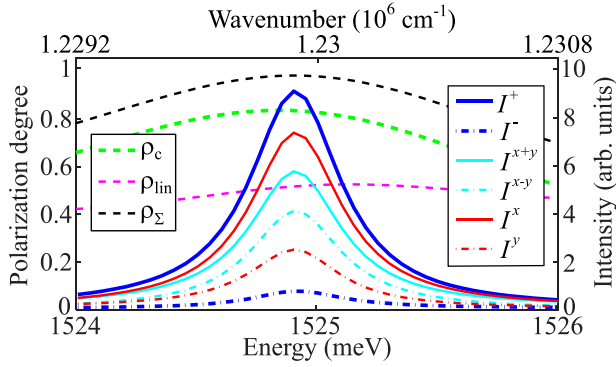


FIG. 3. Calculated (for Sample A) emission intensity spectra in right- and left-circular polarizations (thick blue solid and dashed-dotted lines). The corresponding circular polarization degree spectra are shown by the thick dashed green line. Red and cyan lines show the linearly polarized (in  $xy$  and diagonal directions, respectively) intensities  $I^x, I^y, I^{x+y}, I^{x-y}$ , calculated assuming that all oscillating dipoles are aligned along diagonal  $x+y$  direction. The resulting linear and total polarization degrees  $\rho_{\text{lin}}$  and  $\rho_{\Sigma}$  are shown as magenta and black dashed lines. It can be seen that the linear polarization is predominantly along the  $x$  direction.

emission in right and left circular polarizations, using the optical scattering matrix and Fourier modal method.<sup>10–12,17</sup> In this approximation, the emission is calculated actually for homogeneously distributed oscillating point dipoles in the QW plane, which are driven by external excitation and emit incoherently, so that the intensities rather than the electromagnetic fields are summed up at the receiver. This approximation (so-called weak coupling limit) is not completely valid for describing the lasing. But below and slightly above the threshold of the lasing regime, it might be a reasonable starting point for optimization of the structures.

In this approximation, assuming the overall  $C_4$  symmetry of the system, only a circular polarization of emission can be expected. The linear polarization is absent, because the oscillating dipoles are assumed to be randomly linearly polarized in  $xy$  plane. The calculated emission intensities in right and left circular polarizations  $I^{\pm}$  for a structure with parameters of Sample A are shown in Fig. 3 as blue solid and dashed-dotted lines. The intensities are normalized to the emission intensity of the same oscillating dipoles in vacuum. The resulting dependence of  $\rho_c(\hbar\omega)$  is shown in Fig. 3 by the dashed green line. It can be seen that the emission is expected to be strongly circularly polarized, with  $\rho_c$  up to 80%, in agreement with the experiment. For details on the simulated

linearly polarized components, see our explanations below after discussion of the important features of the circular polarization control by CPC.

Additional insight into the mechanism of circularly polarized emission is provided in Fig. 4 with the calculated spatial distribution of the circularly polarized emission intensity in Sample A at the resonant frequency  $\hbar\omega = 1.522$  eV, as well as the spatial distribution of the DCP of emission  $\rho_c(x, y)$ , over the CPC unit cell. We would like to emphasize that Fig. 4 does not show the emission intensity distributions in a certain plane above the sample, but the spatial distributions of the emission effectiveness from different spatial points of the sample unit cell in the normal direction of the structure. These spatial distributions are connected via the electrodynamic reciprocity principle with the local electric field distributions in the active material plane inside the structure, produced by a normally incident plane wave of the corresponding polarization.<sup>11</sup>

Note that  $\rho_c$  is very sensitive to the etching depth.<sup>12</sup> Figure 5 shows the calculated dependence of the maximum  $\rho_c$  of emission from Samples A (solid line) and B (dashed-dotted line) as functions of etching depth  $N_{\text{etch}}$  (measured in the number of etched Bragg pairs). Thus, the structures employed in our experiments with  $N_{\text{etch}} \sim 4.75$  are in agreement with these calculations, corresponding to the maxima of the expected  $\rho_c$ .

It can be seen in Fig. 2 shows that the measured emission in the lasing mode shows as well a pronounced linear polarization along  $x$  direction in Fig. 1(c), i.e., along the (110) crystallographic direction of the AlGaAs and GaAs layers. There are two possible explanations: (1) The lasing operation itself, with possible preferential stimulated alignment of oscillating dipoles along a defined polarization direction. (2) The operation of the CPC, where possible fabrication-induced deformation of the CPC structures could lead to a reduced structural symmetry.

Although the lasing operation is not included in the simulation model, it is possible to check the effect of possible preferential alignment of oscillating dipoles. Red and cyan lines in Fig. 3 show the calculated emission intensities  $I^{x,y}, I^{x\pm y}$  in linear  $xy$  and diagonal polarizations, assuming that all oscillating dipoles are aligned along diagonal  $x+y$  direction. The linear polarization degree  $\rho_{\text{lin}}$  and total polarization degree  $\rho_{\Sigma}$  are shown as magenta and black dashed lines in Fig. 3. It is seen that the alignment of the oscillating dipoles leads to a pronounced linear  $x$  polarization, as in the experiment.

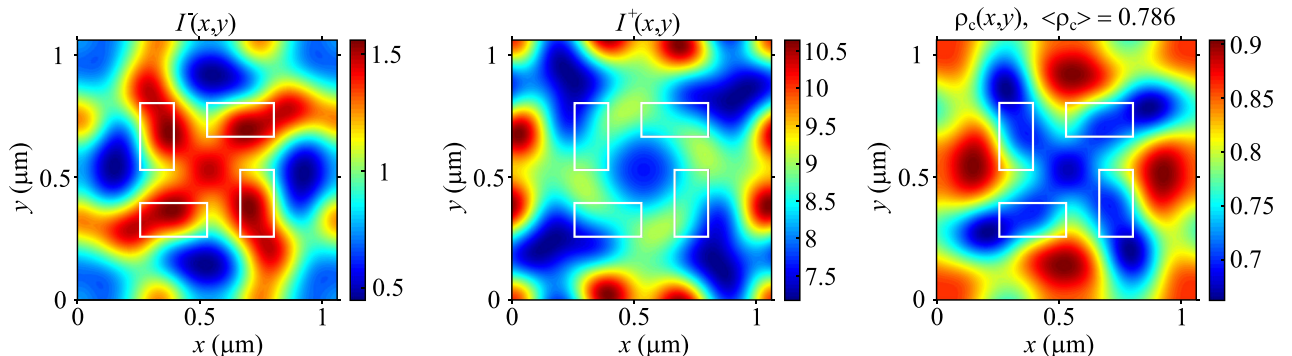


FIG. 4. Calculated spatial emission intensity distributions in Sample A in left ( $I^-(x, y)$ ) and right ( $I^+(x, y)$ ) circular polarizations (left and central panels), and spatial distribution of circular polarization degree  $\rho_c(x, y)$  (right panel).

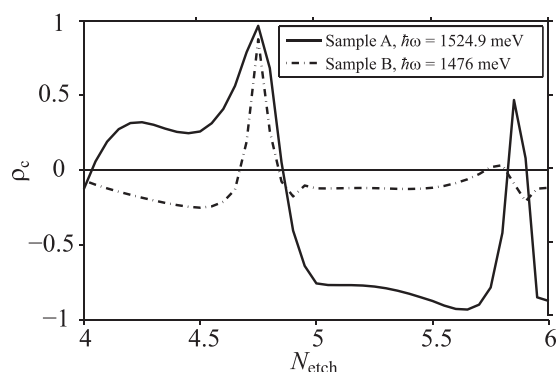


FIG. 5. Calculated dependence of maximum circular polarization degree  $\rho_c$  on etching depth  $N_{etch}$  (measured as the number of etched Bragg pairs) for Sample A (solid line) and Sample B (dashed-dotted line) structures.

As to the possible fabrication-induced deformation of the CPC structures, they may cause the linear polarization of emission as well, see the [supplementary material](#). However, the DCP in this case is usually less than in the perfect structure.

To conclude, we have found that fabricating chiral photonic crystals with light emitting GaAs quantum wells inside a planar MC allows to realize lasing with a high degree of circular polarization of the light emission in the absence of a magnetic field. The advantage of using the CPCs with a large contrast of dielectric permittivities is its giant optical activity. This allows one to fabricate a very thin “waveplate,” with a thickness of the order of the emitted light wavelength. One more advantage of CPC half-wave plates lies in the fact that they, unlike the traditional ones, have in-plane rotational isotropy due to the  $C_4$  symmetry. Thus, our chiral structures do not require linearly polarized emission of the active material at some precise polarization direction, which is an important advantage of the demonstrated approach over conventional quarter-wave plates.

See [supplementary material](#) for a more detailed description of the cavity design and the influence of possible

fabrication-induced deformation of the CPC structures on the linear polarization of emission.

This work has been funded by Russian Scientific Foundation (Grant No. 14-12-01372) and State of Bavaria. We are grateful to K. Konishi, L. Kuipers, M. Kuwata-Gonokami, R. Oulton, H. Tamaru, and F. Capasso for fruitful discussions, and M. Emmerling for preparing the nanopillars.

- <sup>1</sup>E. Yablonovitch, *Phys. Rev. Lett.* **58**, 2059 (1987).
- <sup>2</sup>S. Fan, P. R. Villeneuve, J. Joannopoulos, and E. F. Schubert, *Phys. Rev. Lett.* **78**, 3294 (1997).
- <sup>3</sup>E. Miyai, K. Sakai, T. Okano, W. Kunishi, D. Ohnishi, and S. Noda, *Nature* **441**, 946 (2006).
- <sup>4</sup>A. Papakostas, A. Potts, D. M. Bagnall, S. L. Prosvirnin, H. J. Coles, and N. I. Zheludev, *Phys. Rev. Lett.* **90**, 107404 (2003).
- <sup>5</sup>M. Kuwata-Gonokami, N. Saito, Y. Ino, M. Kauranen, K. Jefimovs, T. Vallius, J. Turunen, and Y. Svirko, *Phys. Rev. Lett.* **95**, 227401 (2005).
- <sup>6</sup>D.-H. Kwon, P. L. Werner, and D. H. Werner, *Opt. Express* **16**, 11802 (2008).
- <sup>7</sup>N. Liu, H. Liu, S. Zhu, and H. Giessen, *Nat. Photonics* **3**, 157 (2009).
- <sup>8</sup>M. Hentschel, L. Wu, M. Schäferling, P. Bai, E. P. Li, and H. Giessen, *ACS Nano* **6**, 10355 (2012).
- <sup>9</sup>X. Yin, M. Schäferling, B. Metzger, and H. Giessen, *Nano Lett.* **13**, 6238 (2013).
- <sup>10</sup>A. A. Maksimov, I. I. Tartakovskii, E. V. Filatov, S. V. Lobanov, N. A. Gippius, S. G. Tikhodeev, C. Schneider, M. Kamp, S. Maier, S. Höfling, and V. D. Kulakovskii, *Phys. Rev. B* **89**, 045316 (2014).
- <sup>11</sup>S. V. Lobanov, T. Weiss, N. A. Gippius, S. G. Tikhodeev, V. D. Kulakovskii, K. Konishi, and M. Kuwata-Gonokami, *Opt. Lett.* **40**, 1528 (2015).
- <sup>12</sup>S. V. Lobanov, S. G. Tikhodeev, N. A. Gippius, A. A. Maksimov, E. V. Filatov, I. I. Tartakovskii, V. D. Kulakovskii, T. Weiss, C. Schneider, J. Geßler, M. Kamp, and S. Höfling, *Phys. Rev. B* **92**, 205309 (2015).
- <sup>13</sup>K. Konishi, M. Nomura, N. Kumagai, S. Iwamoto, Y. Arakawa, and M. Kuwata-Gonokami, *Phys. Rev. Lett.* **106**, 057402 (2011).
- <sup>14</sup>N. Shitrit, I. Yulevich, E. Maguid, D. Ozeri, D. Veksler, V. Kleiner, and E. Hasman, *Science* **340**, 724 (2013).
- <sup>15</sup>P. Rauter, J. Lin, P. Genevet, S. P. Khanna, M. Lachab, A. Giles Davies, E. H. Linfield, and F. Capasso, *Proc. Natl. Acad. Sci.* **111**, E5623 (2014).
- <sup>16</sup>K. Konishi, B. Bai, X. Meng, P. Karvinen, J. Turunen, Y. P. Svirko, and M. Kuwata-Gonokami, *Opt. Express* **16**, 7189 (2008).
- <sup>17</sup>D. M. Whittaker and I. S. Culshaw, *Phys. Rev. B* **60**, 2610 (1999).